



# Ultrafast energy transfer dynamics of phycobilisome from *Thermosynechococcus vulcanus*, as revealed by ps fluorescence and fs pump-probe spectroscopies

Yuma Hirota<sup>1</sup> · Hiroki Serikawa<sup>1</sup> · Keisuke Kawakami<sup>2</sup> · Masato Ueno<sup>3</sup> · Nobuo Kamiya<sup>4</sup> · Daisuke Kosumi<sup>5</sup>

Received: 6 January 2021 / Accepted: 4 May 2021 / Published online: 17 May 2021  
© The Author(s), under exclusive licence to Springer Nature B.V. 2021

## Abstract

Cyanobacterial photosynthetic systems efficiently capture sunlight using the pigment-protein megacomplexes, phycobilisome (PBS). The energy is subsequently transferred to photosystem I (PSI) and II (PSII), to produce electrochemical potentials. In the present study, we performed picosecond (ps) time-resolved fluorescence and femtosecond (fs) pump-probe spectroscopies on the intact PBS from a thermophilic cyanobacterium, *Thermosynechococcus vulcanus*, to reveal excitation energy transfer dynamics in PBS. The photophysical properties of the intact PBS were well characterized by spectroscopic measurements covering wide temporal range from femtoseconds to nanoseconds. The ps fluorescence measurements excited at 570 nm, corresponding to the higher energy of the phycocyanin (PC) absorption band, demonstrated the excitation energy transfer from the PC rods to the allophycocyanin (APC) core complex as well as the energy transfer in the APC core complex. Then, the fs pump-probe measurements revealed the detailed energy transfer dynamics in the PC rods taking place in an ultrafast time scale. The results obtained in this study provide the full picture of the funnel-type excitation energy transfer with rate constants of  $(0.57 \text{ ps})^{-1} \rightarrow (7.3 \text{ ps})^{-1} \rightarrow (53 \text{ ps})^{-1} \rightarrow (180 \text{ ps})^{-1} \rightarrow (1800 \text{ ps})^{-1}$ .

**Keywords** Phycobilisome · Energy transfer · Ultrafast spectroscopy · Excited state dynamics · Fluorescence

## Abbreviations

PBS Phycobilisome  
PSII Photosystem II  
PC Phycocyanin  
APC Allophycocyanin

PSI Photosystem I  
PCB Phycocyanobilin  
OCP Orange carotenoid protein  
*T. vulcanus* *Thermosynechococcus vulcanus*  
IRF Instrument response function  
DAFS Decay-associated fluorescence spectra  
EAFS Evolution-associated fluorescence spectra  
DADS Decay-associated difference spectra  
EADS Evolution-associated difference spectra

✉ Keisuke Kawakami  
keisuke.kawakami@riken.jp

✉ Daisuke Kosumi  
kosumi@kumamoto-u.ac.jp

<sup>1</sup> Department of Physics, Graduate School of Science and Technology, Kumamoto University, 2-39-1 Kurokami, Chuo-ku, Kumamoto 860-8555, Japan

<sup>2</sup> Biostructural Mechanism Laboratory, RIKEN Spring-8 Center, 1-1-1, Sayo, Kouto, Hyogo 679-5148, Japan

<sup>3</sup> Department of Physics, Faculty of Science, Kumamoto University, 2-39-1 Kurokami, Chuo-ku, Kumamoto 860-8555, Japan

<sup>4</sup> The OCU Research Center for Artificial Photosynthesis, Osaka City University, 3-3-138, Sugimoto, Sumiyoshi-ku, Osaka 558-8585, Japan

<sup>5</sup> Institute of Industrial Nanomaterials, Kumamoto University, 2-39-1 Kurokami, Chuo-ku, Kumamoto 860-8555, Japan

## Introduction

Cyanobacteria utilize sunlight energy to split water molecules, releasing oxygen molecules necessary for the growth and development of aerobic organisms. The amount of solar radiation, which is one of the key requirements for photosynthesis, always changes considerably (Kromdijk et al. 2016). When photosynthetic organisms undergo photo-inhibition under high-light irradiation conditions, photosynthetic apparatus dissipates excess of absorbed energy as heat to protect their organisms (Bishop et al. 2007; Karapetyan 2007; Li et al. 2009; Muller et al. 2001). On the other hand, because

sunlight is often dilute for oxygenic photosynthetic reactions even on sunny days, photosynthetic apparatus requires highly efficient light-harvesting ability to capture a large number of photon (Blankenship 2014; Hohmann-Marriott and Blankenship 2011).

Phycobilisome (PBS) is attached to the cytoplasmic surface of thylakoid membrane and is one of the pigment-protein megacomplexes that efficiently capture light and supply energy to the photosynthetic membrane proteins photosystem I and II (PSI and PSII) to convert light energy to chemical potentials (Adir et al. 2020; Grossman et al. 1993; Stadnichuk et al. 2015a; Watanabe and Ikeuchi 2013). PBS typically consists of peripheral phycocyanin (PC) rods projecting radially from central allophycocyanin (APC) core complexes. APC core and PC rod consist of phycobiliproteins and linker proteins, involving photosynthetic pigment of phycocyanobilin (PCB). A heterodimer of the two different  $\alpha$ - and  $\beta$ -subunits of phycobiliprotein forms into the trimeric structure which is the basic unit for the PBS structure (Watanabe and Ikeuchi 2013). PC rod and APC core have the cylindrical structures and cylinders are a stack of trimeric structures of the  $\alpha\beta$ -subunits (MacColl 1998, 2004). The peripheral PC rods initially absorb light in the green–red region of the spectrum and funnel to the APC cores (Bryant and Canniffe 2018; Glazer et al. 1985; Watanabe and Ikeuchi 2013; Yamanaka and Glazer 1980). The high-resolution crystal structures of the isolated PC and APC protein complexes have been reported (Adir et al. 2001; David et al. 2011; Marx and Adir 2013; Peng et al. 2014; Stec et al. 1999; Tang et al. 2015). Further, the overall structures of the intact PBS have been resolved by cryo-electron microscopy (Chang et al. 2015; David et al. 2014; Ma et al. 2020; Zhang et al. 2017) and a structural model of PBS and photosystems was also proposed by a combination of biochemical and spectroscopic methods (Liu et al. 2013). These works clarified the open question how the energies of photosynthetic pigments bound to phycobiliprotein are modulated by surrounding protein environments.

Photophysical properties of individual phycobiliprotein, intact PBS, and PBS-PS super-complex have been investigated by various spectroscopic methods (Collini et al. 2010; Glazer et al. 1985; Ho et al. 2020; Holzwarth et al. 1987; Liu et al. 2013; MacColl 2004; Maxson et al. 1989; Nganou et al. 2015; Niedzwiedzki et al. 2019; Pieper et al. 2017; Sandström et al. 1988; Tian et al. 2012; van Stokkum et al. 2018; Wahadoszamen et al. 2020; Wang and Moerner 2015; Womick and Moran 2009; Zhang et al. 1997). In the early stage of investigations on PBS, spectroscopic measurements were performed on the isolated PC and APC monomer/oligomer and complexes to characterize their photophysical properties and excited state dynamics (Glazer et al. 1985; Holzwarth et al. 1987; MacColl 2004; Maxson et al. 1989; Sandström et al. 1988). Investigations on the individual PC

and APC subunits have been extended to single molecule spectroscopy (Gwizdala et al. 2016; Wang and Moerner 2015) and observations of the electronic coherence between chromophores in PC and APC (Womick and Moran 2009). PBS in cells were also investigated by time-resolved spectroscopy to clarify energy supply from PBS to PSII or PSI and energy dissipation (Petrasek et al. 2005; Tian et al. 2011). The cyanobacterium *Synechocystis* PCC 6803 has a hemi-discoidal-type PBS megacomplex and has been intensively investigated by spectroscopic measurements because this species has orange carotenoid protein (OCP) acting as an energy dissipation to protect photosystems from excess of absorbed energy (Akimoto et al. 2014; Tian et al. 2012, 2011). The cyanobacterium *Acaryochloris mariana* described in 1996 has a single rod-type PBS consisting of the PC and APC trimers and the energy transfer dynamics in the rod-type PBS have been reported (Ho et al. 2020; Nganou et al. 2015; Niedzwiedzki et al. 2019; Petrasek et al. 2005; Pieper et al. 2017), while it has been argued that PBS from *Acaryochloris mariana* is absent or scarcity of APC (Bar-Zvi et al. 2018). Phycobiliproteins from cryptophytes are broadly classified as PC or phycoerythrin heterodimers that bind eight bilins. Even though phycobiliproteins from cryptophytes do not form megacomplexes such as PBS, strongly interacted heterogeneous chromophores (PCB, phycoerythrobilin and dihydrobiliverdin) show electronic coherence and efficient energy transfer (Collini et al. 2010; Wong et al. 2012).

Despite many works on PBS, the details of energy funnels of overall PBS have not been sufficiently elucidated yet. Therefore, it has been still matter of controversy how PBS efficiently absorbs and transfers light energy to PS, how PBS interacts to PS, and how PBS regulates excess energy under high light conditions. In the present study, we isolated the intact PBS from the thermophilic cyanobacterium, *Thermosynechococcus vulcanus* (*T. vulcanus*), and performed ps time-resolved fluorescence and femtosecond fs pump-probe spectroscopic measurements on the intact PBS to reveal energy transfer dynamics. *T. vulcanus* has a hemi-discoidal-type PBS megacomplex similar to *Synechocystis* PCC 6803 and its excitation energy transfer dynamics probed by femtosecond pump-probe spectroscopy has been reported (Nganou et al. 2016). However, the previous study was performed in the limited spectral and temporal ranges. Thus, the excitation energy transfer dynamics in PBS, such as those in the PC and APC monomers/trimers, in the PC rods, among the PC rod and the APC core, and in the APC cores was insufficiently understood. Here, the energy transfer dynamics of the intact PBS were well characterized in detailed by spectroscopic techniques covering the wide temporal range from femtosecond to nanosecond upon excitation at 570 nm, corresponding to the higher energy of the PC absorption band.

## Experimental

### Sample preparation

*T. vulcanus* cells (5.0 L flasks  $\times$  6 pieces) were cultured in a phosphate medium (Kawakami and Shen 2018; Shen et al. 2011). Obtained cells were disrupted by lysozyme treatment and a freeze-thawing method. The disrupted samples (thylakoid membranes) in a high-concentration phosphate buffer containing 0.8 M  $\text{KH}_2\text{PO}_4$  (pH 6.8) at a chlorophyll concentration of 2.0 mg/mL were solubilized with the same volume of 4.0% (w/v) Triton X-100 in the phosphate buffer for 30 min on ice under a dark condition. The high-concentration phosphate buffer containing 0.8 M  $\text{KH}_2\text{PO}_4$  (pH 6.8) was used in all sample preparation steps to stabilize the overall structure of PBS (Chang et al. 2015). Subsequently, the samples were centrifuged (38,600  $\times$  g, 90 min, 4 °C) to remove the unsolubilized cells, and the obtained supernatants were subjected to 0–1.0 M trehalose density gradient ultracentrifugation (104,000  $\times$  g, 15 h, 4 °C). After ultracentrifugation, the obtained PBS solutions were concentrated using ultrafiltration (Amicon Ultra15, 100 KMWCO; Millipore) and stored at – 80 °C. The isolated PC trimer and the APC core complex solutions were obtained by subjecting the obtained PBS to trehalose density gradient ultracentrifugation containing 0.3 M  $\text{KH}_2\text{PO}_4$  (pH 6.8) (Barber et al. 2003) (see the Supplementary Information). The PC trimer is composed of the heterodimer of the PC  $\alpha$  and  $\beta$ -subunits called as CpcA and CpcB those have one ( $\alpha$ -C84) and two ( $\beta$ -C84 and  $\beta$ -C155) PCB molecules, respectively. The obtained APC core complex is considered to be comprised A1 and A2-cylinders (mainly ApcA, ApcB, ApcD, ApcE, and ApcF subunits) and B-cylinder (mainly ApcA and ApcB subunits) (Kawakami et al. 2021).

### ps Fluorescence measurement

The ps time-resolved fluorescence measurements were performed by a 1 kHz Ti:Sapphire regenerative amplifier (Spectra Physics, Spitfire-Pro) and a time-correlated single photon counting (TCSPC) system. The visible excitation pulses with a repetition rate of 1 kHz were obtained from an optical parametric amplifier (Spectra Physics, TOPAS-C). The fluorescence of the sample at the right angle to the excitation beam was detected by a single photon avalanche diode (MPD, PD-050-CTD) through a spectrometer (Acton Research, SP275i). The detected photon signals were taken by the TCSPC module (Becker & Hickles, SPC130EM) (Yamamoto et al. 2020). Relative polarization between the excitation pulse and the detected fluorescence was set to

a magic angle of 54.7°. The excitation wavelength was set to 570 nm for the intact PBS and isolated PC and to 650 nm for the isolated APC. The excitation intensity was set to 1.0 nJ/pulse. The instrumental response function of the system was about 20 ps. The fluorescence kinetics of the samples were measured ranging from 600 to 780 nm with a 10 nm step. The samples were packed in a static cuvette with a 10 mm optical length. The steady-state fluorescence spectra of the samples were obtained by a time-integral of fluorescence signals detected at each wavelength. The measurements were performed at room temperature (296 K).

### fs Pump-probe measurement

The femtosecond pump-probe spectroscopic measurements have been described in detail elsewhere (Kosumi et al. 2010). The visible excitation pulse was obtained from an optical parametric amplifier. The excitation wavelength and intensity were set to 570 nm and 2.0 nJ/pulse, respectively. The white light continuum probe pulses, generated using a 2.0 mm sapphire plate, were detected by a CMOS linear image sensor (Hamamatsu Photonics K. K., S12198-1024Q) through a spectrometer (Shimadzu Corp., P0380-01). The excitation pulse was modulated at 500 Hz by an optical chopper and the data output was synchronized with a laser repetition rate of 1 kHz (Kojima et al. 2020; Kosumi et al. 2010). The relative polarization between the excitation and probe pulses was set to be magic angle of 54.7°. The instrumental response function and the precise zero-time delay were determined by the cross-correlation between excitation and probe pulses. After a chirp compensation, the uncertainty in the zero-time delay was less than 10 fs. The sample was packed in a static cuvette with a 2.0 mm optical length and was stirred by a micro magnetic bar in the cuvette to avoid optical damage. The measurements were performed at room temperature (296 K).

## Results and discussion

Figure 1 shows the steady-state absorption spectra of the intact PBS and the isolated PC trimer and APC core complex at room temperature. The absorption band of the intact PBS peaked at 620 nm, which is due to the one photon electronic transition from the ground state to the lowest-lying singlet excited state of PCB bound to the phycobiliprotein complexes. When comparing the absorption spectra of the isolated PC trimer and the intact PBS, the APC contribution can be seen as a broadening on the red-side of the main peak even in high inhomogeneity at room temperature. Therefore, to observe overall PC  $\rightarrow$  APC energy transfer dynamics in PBS, we selected the excitation wavelength to be 570 nm,

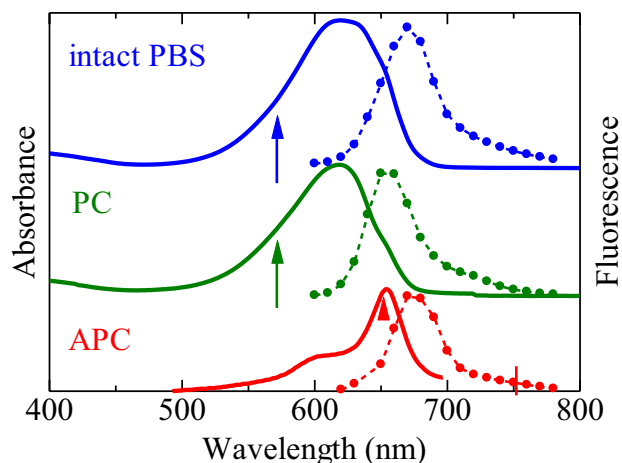


**Fig. 1** The steady-state absorption and time-integrated fluorescence spectra of the intact PBS and the isolated PC trimer and APC core complex at room temperature. Arrows indicate excitation wavelengths for fluorescence measurements. Broken lines are interpolations by a polynomial function

which corresponds to the blue-side of the PC absorption band. The steady-state fluorescence spectra of the samples obtained by ps fluorescence measurements at room temperature are also plotted in Fig. 1. The observed fluorescence spectrum of the intact PBS excited at 570 nm has a narrower feature than the absorption spectrum. The peak of the intact PBS fluorescence was located at 670 nm, which was consistent with the fluorescence spectrum of the APC core complex as shown in Fig. 1 (Jallet et al. 2012; Liu et al. 2013; Stadnichuk et al. 2015b; Tang et al. 2015). Thus, the results suggest the PC → APC energy transfer of the intact PBS after the excitation into the PC absorption band at 570 nm.

Figure 2 presents (a) the time-wavelength 2D map of fluorescence and (b) the kinetic traces of the fluorescence from the intact PBS excited at 570 nm. The solid lines in Fig. 2b are the best-fit curves for the rise and decay phases convoluted with the instrument response function (IRF). The observed fluorescence kinetics of the intact PBS depends strongly on the detection wavelength. At the shorter detection wavelength (below 640 nm), the fluorescence signals instantaneously rise and quickly decays. On the other hand, fluorescence detected at the longer wavelength slowly rises and has the longer lifetime. We globally analyzed the obtained fluorescence kinetics traces, and then three exponential components were required to fit the kinetics traces fully. Time-constants of each exponential component were determined to be 50 ps, 180 ps, and 1.8 ns.

To visualize the detailed energy transfer dynamics in PBS, we show the decay-associated fluorescence spectra (DAFS) of the intact PBS excited at 570 nm in Fig. 3a. The data are plotted by dots and the lines are interpolated by a polynomial function. The longest decay DAFS of 1.8 ns was

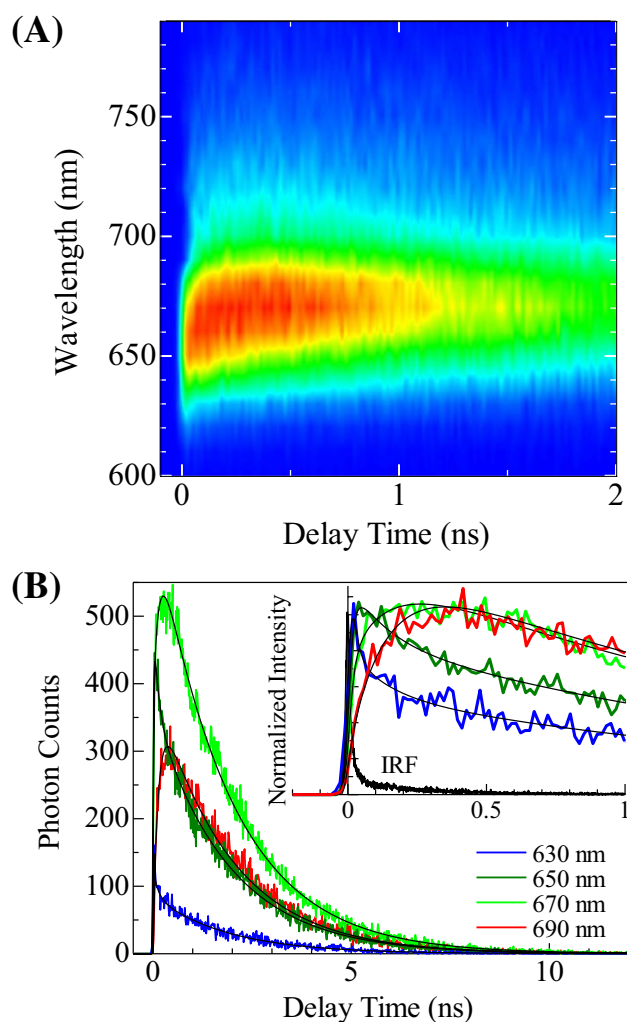


**Fig. 2** a Time-wavelength 2D map of fluorescence and b kinetic traces of fluorescence of the intact PBS given by excitation at 570 nm. The thin solid lines are the best-fit curves

obtained as a positive phase in all spectral regions. Conversely, the first (50 ps) and second (180 ps) DAFS exhibit both negative and positive phases. Therefore, the exponential components with the time constants of 50 and 180 ps appear as decays at shorter detected wavelengths and as rises at longer wavelengths in the kinetic traces as shown in Fig. 2b.

The evolution-associated fluorescence spectra (EAFS) of the intact PBS excited at 570 nm shown in Fig. 3b were also obtained by a global analysis based on a sequential irreversible model:  $(50 \text{ ps})^{-1} \rightarrow (180 \text{ ps})^{-1} \rightarrow (1.8 \text{ ns})^{-1}$ . The second EAFS with the time-constant of 180 ps have the fluorescence peak around 660 nm, corresponding to the fluorescence of the isolated APC trimer comprised the ApcA and ApcB subunits (Wang and Moerner 2015). Thus, the second EAFS is likely to be assigned to the APC trimer comprised the ApcA and ApcB subunits in the APC core complex. The third EAFS with the longest decay time-constant of 1.8 ns

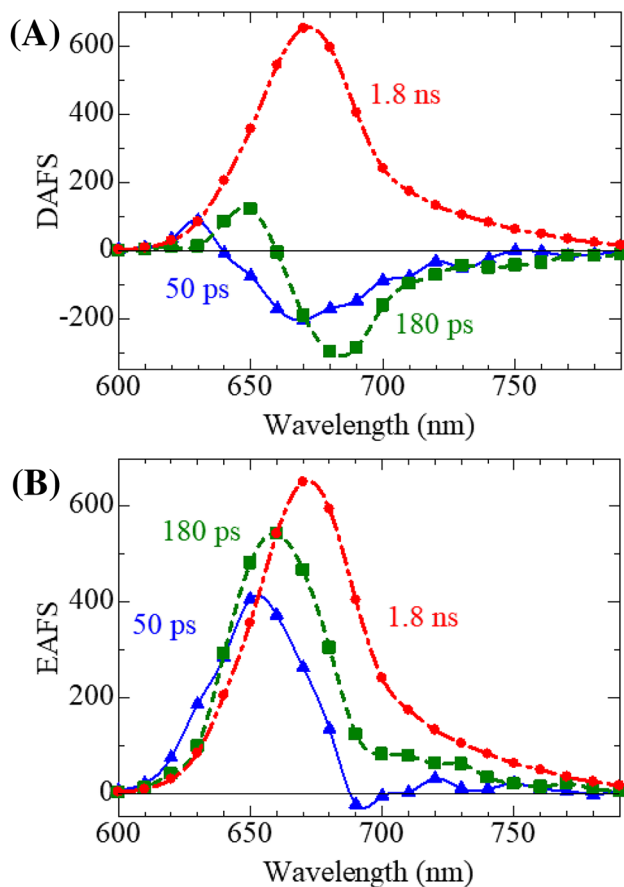


**Fig. 3** **a** Decay-associated fluorescence spectra and **b** Evolution-associated fluorescence spectra of the isolated PBS excited at 570 nm. Lines are interpolations by a polynomial function

peaks at 670 nm, corresponding to the previously reported fluorescence spectra of the terminal emitter subunits in the APC core complex (Jallet et al. 2012; Liu et al. 2013; Stadnichuk et al. 2015b; Tang et al. 2015). In *T. vulcanus*, genes coding for the terminal emitter subunits ApcD, ApcE and ApcF were detected, and we identified these subunits in PBS from *T. vulcanus* by mass spectrometry and N-terminal sequence analyzes (Kawakami et al. 2021). Therefore, the third EAFS is assignable to the fluorescence of terminal emitter subunits (ApcD, ApcE and ApcF) in the APC core complex. The first EAFS with the time-constant of 50 ps peaks around 650 nm. It has been reported that the energy transfer from the PC rods to the APC core takes place within a 40–500 ps timescale (Liu et al. 2013; Tian et al. 2012, 2011; Zhang et al. 1997). Liu et al. have reported to be 340 ps for the energy transfer in the isolated PC rods and to be 430 ps for the PC → APC energy transfer in the isolated PBS at 77 K (Liu et al. 2013). The energy transfer time-constants have also been reported to be 6 and 77 ps at 77 K for PBS in an intact cell from *Synechocystis* sp. PCC 6803 (Tian et al. 2011). These results imply that the first EAFS is

associated with the PC trimer interacting with the APC core complex. The first EAFS was observed at a peak wavelength of 650 nm, slightly red-shifted compared with the isolated PC fluorescence (~645 nm) (Gwizdala et al. 2018; Liu et al. 2013). However, it is likely that the fluorescence peak of the PC rods in PBS is longer than that of the isolated PC trimer because of the interaction between the PC trimers and/or between the PC trimer and the APC trimer. Therefore, the first EAFS potentially originates from the PC fluorescence. The obtained time-constants of 50 and 180 ps should be assigned to the energy transfer times of the PC rods → the ApcA /ApcB subunits in the APC core complex and the ApcA/ApcB subunits → terminal emitter subunits (ApcD, ApcE and ApcF) in the APC core complex. These observations strongly suggest that the isolated intact PBS maintains the megacomplex without any dissociation and demonstrates the energy migration processes from the photo-excited PC rods to the terminal emitters (ApcD, ApcE, and ApcF) via the ApcA/ApcB subunits in the APC core complex.

To clarify the detailed energy transfer dynamics of PBS occurring in an ultrafast timescale, we performed fs pump-probe spectroscopy on the intact PBS at room temperature. The photo-induced absorption spectra shown in Fig. 4a were recorded after the excitation at 570 nm corresponding to the blue-side of the PC absorption band in the intact PBS. Figure 4b shows the kinetic traces of the absorbance changes of the intact PBS obtained by fs pump-probe spectroscopic measurements. The negative absorbance changes include both the ground state bleaching and the stimulated emission of PCB bound to the PC and APC protein complexes. The positive signal appeared in the kinetic trace probed at 670 nm is assigned to the transient absorption due to the excited state of PCB. The trace probed at 610 nm instantaneously rises and decays within a hundred picosecond. On the other hand, the kinetic traces probed at 650 and 670 nm rise exponentially. Thus, the data imply the ultrafast excitation energy transfer in PBS taking place in a picosecond timescale.

The solid lines in Fig. 4b are the best-fit curves for the rise and decay phases convoluted with the instrument response function assuming a Gaussian temporal profile. The obtained kinetics traces of the photo-induced absorbance changes were analyzed globally, and then five exponential components were required to fit the kinetics traces fully. The decay-associated difference spectra (DADS) of the intact PBS excited at 570 nm are plotted in Fig. 5a. In our fs pump-probe measurements, the delay time is limited up to 1.2 ns. Then, the absorbance change probed at 670 nm remains even after more than 1.2 ns as shown in Fig. 4, indicating that the longer time-constants, as observed in our ps fluorescence measurements, cannot be properly determined by fs pump-probe measurements. Therefore, we used the time-constants of 180 ps and 1.8 ns determined by ps fluorescence

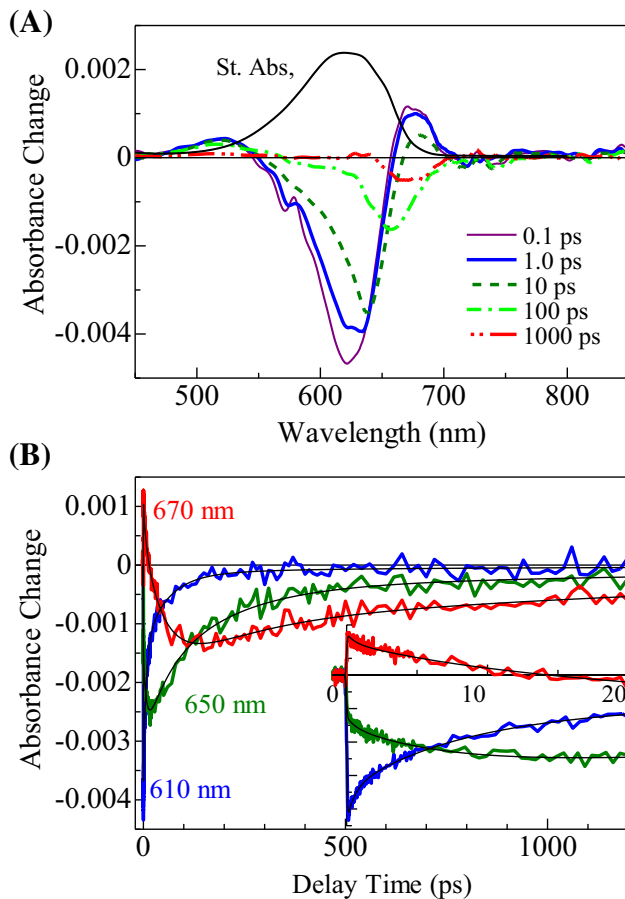


**Fig. 4** **a** Photo-induced absorption spectra and **b** their kinetic traces of the intact PBS after the excitation at 570 nm

measurements during the analysis on the fs pump-probe data. The negative absorbance changes exhibit both the ground state bleaching and stimulated emission. The negative peaks shift to longer wavelength with an increase of the decay time-constants. In the fs pump-probe measurement of the intact PBS, the observed signals are mainly negative part corresponding to the ground state bleaching and stimulated emission. Thus, negative part of DADS represents decay of the signal (recovery of absorption bleaching here) while positive part corresponds to rise of signal elsewhere (onset of bleaching there) with the same time constant. However, in addition to the main negative signals, the positive signals (tentatively assigned to the transient absorption of PCB) were also observed in the photo-induced absorption spectra as shown in Fig. 4a, whereas their amplitudes are small (see also Fig. S2 in the Supplementary information). Therefore, the positive changes in DADS mean mainly the rise of the bleaching and stimulated emission signals and partly the decay of the transient absorption. In addition to the two longer decay components of 180 ps and 1.8 ns, the third DADS (53 ps) agrees well with the first DAFS (EAFS) with

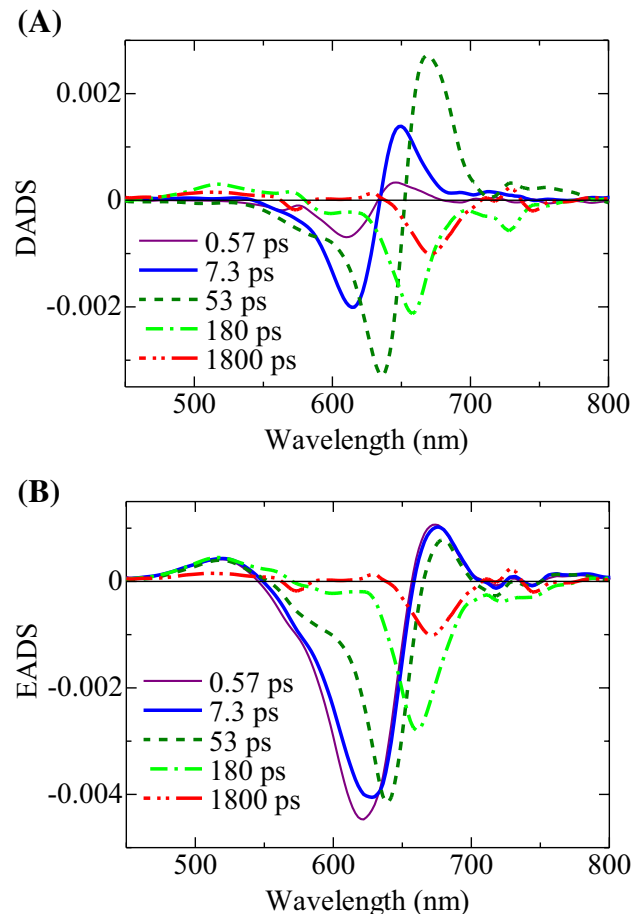


**Fig. 5** **a** Decay-associated and **b** evolution-associated difference spectra of the intact PBS excited at 570 nm

the decay time-constant of 50 ps observed by ps fluorescence measurements. Further, the two faster decay components with the time-constants of 0.53 and 7.3 ps were observed in the fs pump-probe measurements.

For the simple description of the energy transfer dynamics of the intact PBS, the observed kinetics of the photo-induced absorption were analyzed globally based on a sequential irreversible model,  $(0.57 \text{ ps})^{-1} \rightarrow (7.3 \text{ ps})^{-1} \rightarrow (53 \text{ ps})^{-1} \rightarrow (180 \text{ ps})^{-1} \rightarrow (1800 \text{ ps})^{-1}$ . It is possible that due to spatial complexity of the PBS some energy transfer steps happen simultaneously and may not be simply deduced from sequential fitting that is more like presentation of the spectral evolution of the whole system over time. In addition, due to the broad absorption spectrum of the PC rods it is likely that 570 nm excitation will initially excite more than one spectral species, and that process simply may not be reflected in a sequential pattern. Nevertheless, the evolution-associated difference spectra (EADS) based on a simple sequential relaxation scheme give more information about the origin of decay components and the time-evolution of the whole system. Therefore, we hereafter discuss the energy transfer

dynamics of the intact PBS on the basis of EADS instead of more realistic but complicated kinetic model (another model is described in the “Supplementary Information”). Figure 5b shows EADS spectra of the intact PBS excited at 570 nm. The first EADS (0.57 ps) has the negative band peaked at 620 nm corresponding to the steady-state absorption peak of the isolated PC as shown in Fig. 1. The second EADS is similar spectral feature to the first EADS, even though the absorption band of the second EADS (7.3 ps) becomes narrower and its peak shifts to 10 nm longer wavelength compared with the first EADS. Thus, the first and second EADS can be associated with the PC rods. The negative band of the third EADS (53 ps) exhibits the negative peak at 640 nm and a pronounced narrower shape. The peak wavelength of 640 nm for the third EADS is longer than the isolated PC absorption band but shorter than the absorption band of the isolated APC core complex. However, as mention above, it is likely that the absorption peak of the PC rods in PBS is longer than that of the isolated PC trimer because of the interaction between the PC and APC subunits. Then, the spectral structure of the third EADS is similar to those for the first and second EADS having negative and positive absorption bands. Therefore, the third EADS is assignable to the PC rods. Indeed, the steady-state absorption spectrum of the isolated PC trimer has a red-shoulder as shown in Fig. 1. This absorption band corresponds to the third EADS (53 ps) centered at 640 nm. Then, Gwizdala et al. has recently reported the red-form PC of *Synechocystis* PCC 6803 that is involved in direct energy transfer to PSI (Gwizdala et al. 2018). The presence of any CpcG subunit stabilizes one or the other conformation. The PBS from *T. vulcanus* also has the CpcG subunit (Kawakami et al. 2021). Thus, it is likely that the third EADS originates from the red-form PC rod.

The fourth (180 ps) and fifth (1.8 ns) EADS, exhibit the different spectral shapes compared with those of the former three EADS originated from the PC rods, i.e. the absence of the positive absorption band and the pronounced red-shift of the negative band. Thus, the fourth and fifth EADS are assigned to the APC core complex. The negative peak of the fourth EADS (180 ps) is located at 660 nm, corresponding to the absorption band of the isolated APC cores (654 nm) as shown in Fig. 1. On the other hand, the fifth (1.8 ns) EADS have the negative band peaked at 670 nm that is slightly longer wavelength than the steady-state absorption of the isolated APC core. This component is associated with the terminal emitter subunits (ApcD, ApcE, and ApcF), on the basis of the ps fluorescence measurement. Therefore, the time-constant of 180 ps is assigned to the energy transfer from the ApcA/ApcB subunits to the terminal emitters (ApcD, ApcE, and ApcF) in the APC core complex. The absence of the positive absorbance change of the terminal states of PBS have been reported in cyanobacterium *T. vulcanus*, *Acaryochloris marina* and *Synechosystis* PCC 6803

(Nganou et al. 2015, 2016; Niedzwiedzki et al. 2019; van Stokkum et al. 2018). The positive absorption band of PCB appears just below the bleaching signal at earlier delays in the photo-induced absorption spectra. Thus, it is likely that the positive absorbance change is suppressed by the stimulated emission of the PCB bound to the APC core complex that is a strongly emissive character due to surrounding protein environments. On the other hand, Niedzwiedzki et al. demonstrated that the characteristic positive signal around 670 nm could originate from electrochromic effect. The  $\alpha\beta$ -subunits (CpcA and B) of the PC monomer contain three PCB molecules while those of the APC monomer have two PCB molecules (Zilinskas and Greenwald 1986). This can explain the appearance of the positive signal around 670 nm only in the PC rod because closely packed PCB in CpcA and B subunits realizes a stronger interaction between PCB molecules. However, it is difficult in this study to determine whether the positive signal is due to a transient absorption band or electrochromic band-shift, as both show the same temporal dependence.

The energy transfer dynamics of the intact PBS obtained in this study is summarized in Fig. 6. The third EADS (53 ps) exhibits the terminal state of the PC rod interacting with the APC cores, and thus the time-constant of 53 ps associated with the third EADS is assigned to the energy transfer time from the PC rod to the APC core. In the previous study, Nganou et al. claimed the energy transfer from the PC rod to the APC core occurred with the time-constant of 888 fs (Nganou et al. 2016). This time-constant is much faster than that reported previously for the energy transfer from the PC rods to the APC core complex (Liu et al. 2013; Tian et al. 2012, 2011; Zhang et al. 1997). Further, the characteristic spectral feature (negative and positive changes)

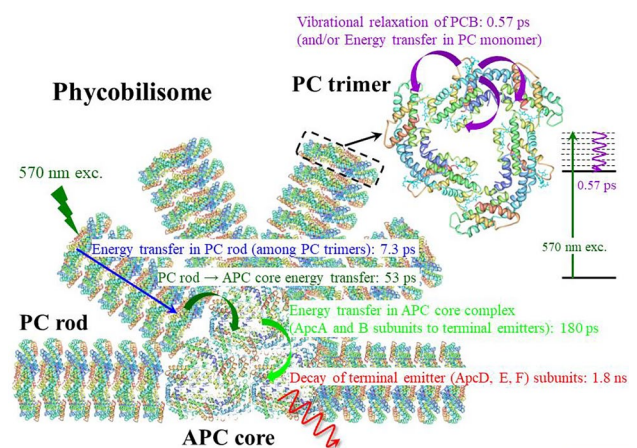


**Fig. 6** A schematic excitation energy transfer model of the intact PBS from *T. vulcanus*. This overall PBS model was drawn referencing the PBS structures from *Anabaena* and *Griffithsia pacifica* (Chang et al. 2015; Zhang et al. 2017)

due to the strong interaction between PCB molecules should be assigned to the PC trimers and rods as discussed above. Thus, we concluded that the third EADS (53 ps) is associated with the energy transfer time from the red-form PC rod to the APC core complex. The time-constant for energy transfer in PC rods has been reported to be in a timescale of several picoseconds (Niedzwiedzki et al. 2019; Tian et al. 2012). Therefore, it is concluded that the time-constant of 7.3 ps obtained in this study originated from the energy transfer in the PC rods (PC trimer → PC trimer). The fastest time-constant of 0.57 ps can be assigned to the vibrational relaxation in PCB bound to the PC subunit (CpcA or B). The 570 nm pulses excited the highly vibrational level of the PCB excited state as shown in Fig. 6. Thus, vibrational relaxation processes can be enhanced in the excited state dynamics. Indeed, the first EADS exhibit blue-shifted comparing with the second EADS (See also Fig. S4 in the “Supplementary Information”). On the other hand, ultrafast energy transfer and electronic quantum coherence have been reported in phycobiliprotein complexes from cryptophyte algae (Collini et al. 2010; Wong et al. 2012). In *T. vulcanus*, the energy transfer between  $\beta$ -C155 (CpcB) and  $\alpha$ -C84 (CpcA)/ $\beta$ -C84 (CpcB) molecules in the PC monomer (CpcA and CpcB subunits) is also possible in a sub-picosecond timescale. The blue-shifted spectrum of the first EADS comparing with the second EADS can be explained by the different protein environments between  $\beta$ -C155 (CpcB) and  $\alpha$ -C84 (CpcA)/ $\beta$ -C84 (CpcB). However, Fig. 5a shows that the amplitude of the first DADS is rather small. Thus, it is more likely that the fastest time-constant originates from the vibrational relaxation of PCB even though we cannot exclude a possibility of the energy transfer in the PC monomer (CpcA/CpcB subunits) taking place in a sub-picosecond timescale.

## Conclusions

In the present study, we isolated the intact PBS megacomplexes from a thermophilic cyanobacterium, *T. vulcanus* and performed ps time-resolved fluorescence and fs pump-probe spectroscopic measurements to reveal the excitation energy transfer dynamics in the intact PBS. The photophysical property and energy transfer dynamics of the intact PBS were well characterized by spectroscopic techniques covering wide temporal range from femtosecond to nanosecond upon excitation at 570 nm, corresponding to the higher energy of the PC absorption band. The ps fluorescence measurements demonstrated the excitation energy transfer of the PC rods → the APC core complex → the terminal emitting subunits in the APC core complex taking place in a timescale from several ten ps to ns. Then, the fs pump-probe measurements revealed the detailed energy transfer dynamics in an

ultrafast time scale such as energy transfer/relaxation in the PC trimer, energy transfer in the PC rod, and energy transfer from the PC rod to the APC core complex. The results obtained by ps fluorescence and fs pump-probe measurements provides the full picture of the funnel-type excitation energy transfer with rate constants of  $(0.57 \text{ ps})^{-1} \rightarrow (7.3 \text{ ps})^{-1} \rightarrow (53 \text{ ps})^{-1} \rightarrow (180 \text{ ps})^{-1} \rightarrow (1800 \text{ ps})^{-1}$ . The results obtained in this study may assist to understand energy transport between PBS and photosystems in primary photosynthetic processes of cyanobacteria and red algae.

**Supplementary Information** The online version contains supplementary material available at <https://doi.org/10.1007/s11120-021-00844-0>.

**Acknowledgements** This work was supported in part by the Grant-in-Aid for Challenging Exploratory Research (No. 16K13863) and Scientific Research on Innovative Areas “Innovations for Light-Energy Conversion (I<sup>4</sup>LEC)” (Nos. 17H06434 and 18H05173). DK thanks Iketani Science and Technology Foundation Research Support (No. 0281020-A). This work was also partly supported by the Joint Usage/Research of Institute of Pulsed Power Science, Kumamoto University (to KK and DK, 2017–2020).

## Declarations

**Conflict of interest** The authors declare that they have no conflicts of interest.

## References

- Adir N, Bar-Zvi S, Harris D (2020) The amazing phycobilisome. *Biochim Biophys Acta* 1861:148047. <https://doi.org/10.1016/j.bbabi.2019.07.002>
- Adir N, Dobrovetsky Y, Lerner N (2001) Structure of c-phycocyanin from the thermophilic cyanobacterium *Synechococcus vulcanus* at 2.5 Å: structural implications for thermal stability in phycobilisome assembly. *J Mol Biol* 313:71–81. <https://doi.org/10.1006/jmbi.2001.5030>
- Akimoto S, Yokono M, Yokono E, Aikawa S, Kondo A (2014) Short-term light adaptation of a cyanobacterium, *Synechocystis* sp. PCC 6803, probed by time-resolved fluorescence spectroscopy. *Plant Physiol Biochem* 81:149–154. <https://doi.org/10.1016/j.plaphy.2014.01.007>
- Bar-Zvi S, Lahav A, Harris D, Niedzwiedzki DM, Blankenship RE, Adir N (2018) Structural heterogeneity leads to functional homogeneity in *A. marina* phycocyanin. *Biochim Biophys Acta* 1859:544–553. <https://doi.org/10.1016/j.bbabi.2018.04.007>
- Barber J, Morris EP, da Fonseca PC (2003) Interaction of the allophycocyanin core complex with photosystem II. *Photochem Photobiol Sci* 2:536–541. <https://doi.org/10.1039/b300063j>
- Bishop CL, Ulas S, Baena-Gonzalez E, Aro EM, Purton S, Nugent JH, Maenpaa P (2007) The PsbZ subunit of photosystem II in *Synechocystis* sp. PCC 6803 modulates electron flow through the photosynthetic electron transfer chain. *Photosynth Res* 93:139–147. <https://doi.org/10.1007/s11120-007-9182-0>
- Blankenship RE (2014) *Molecular mechanisms of photosynthesis*. John Wiley & Sons, Missouri
- Bryant DA, Canniffe DP (2018) How nature designs light-harvesting antenna systems: design principles and functional realization in



- chlorophototrophic prokaryotes. *J Phys B* 51:033001. <https://doi.org/10.1088/1361-6455/aa9c3c>
- Chang L, Liu X, Li Y, Liu CC, Yang F, Zhao J, Sui SF (2015) Structural organization of an intact phycobilisome and its association with photosystem II. *Cell Res* 25:726–737. <https://doi.org/10.1038/cr.2015.59>
- Collini E, Wong CY, Wilk KE, Curmi PM, Brumer P, Scholes GD (2010) Coherently wired light-harvesting in photosynthetic marine algae at ambient temperature. *Nature* 463:644–647. <https://doi.org/10.1038/nature08811>
- David L, Marx A, Adir N (2011) High-resolution crystal structures of trimeric and rod phycocyanin. *J Mol Biol* 405:201–213. <https://doi.org/10.1016/j.jmb.2010.10.036>
- David L, Prado M, Arteni AA, Elmlund DA, Blankenship RE, Adir N (2014) Structural studies show energy transfer within stabilized phycobilisomes independent of the mode of rod-core assembly. *Biochim Biophys Acta* 1837:385–395. <https://doi.org/10.1016/j.bbabi.2013.12.014>
- Glazer AN, Chan C, Williams RC, Yeh SW, Clark JH (1985) Kinetics of energy flow in the phycobilisome core. *Science* 230:1051–1053. <https://doi.org/10.1126/science.230.4729.1051>
- Grossman AR, Schaefer MR, Chiang GG, Collier JL (1993) The phycobilisome, a light-harvesting complex responsive to environmental conditions. *Microbiol Rev* 57:725–749
- Gwizdala M, Berera R, Kirilovsky D, van Grondelle R, Krüger TPJ (2016) Controlling light harvesting with light. *J Am Chem Soc* 138:11616–11622. <https://doi.org/10.1021/jacs.6b04811>
- Gwizdala M, Krüger TPJ, Wahadoszamen M, Gruber JM, van Grondelle R (2018) Phycocyanin: one complex two states, two functions. *J Phys Chem Lett* 9:1365–1371. <https://doi.org/10.1021/acs.jpcclett.8b00621>
- Ho MY, Niedzwiedzki DM, MacGregor-Chatwin C, Gerstenecker G, Hunter CN, Blankenship RE, Bryant DA (2020) Extensive remodeling of the photosynthetic apparatus alters energy transfer among photosynthetic complexes when cyanobacteria acclimate to far-red light. *Biochim Biophys Acta* 1861:148064. <https://doi.org/10.1016/j.bbabi.2019.148064>
- Hohmann-Marriott MF, Blankenship RE (2011) Evolution of Photosynthesis. *Annu Rev Plant Biol* 62:515–548. <https://doi.org/10.1146/annurev-arplant-042110-103811>
- Holzwarth AR, Wendler J, Suter GW (1987) Studies on chromophore coupling in isolated phycobiliproteins. *Biophys J* 51:1–12. [https://doi.org/10.1016/s0006-3495\(87\)83306-4](https://doi.org/10.1016/s0006-3495(87)83306-4)
- Jallet D, Gwizdala M, Kirilovsky D (2012) ApcD, ApcF and ApcE are not required for the orange carotenoid protein related phycobilisome fluorescence quenching in the cyanobacterium *Synechocystis* PCC 6803. *Biochim Biophys Acta* 1817:1418–1427. <https://doi.org/10.1016/j.bbabi.2011.11.020>
- Karapetyan NV (2007) Non-photochemical quenching of fluorescence in cyanobacteria. *Biochemistry* 72:1127–1135. <https://doi.org/10.1134/s0006297907100100>
- Kawakami K, Shen JR (2018) Purification of fully active and crystallizable photosystem II from thermophilic cyanobacteria. *Methods Enzymol* 613:1–16. <https://doi.org/10.1016/bs.mie.2018.10.002>
- Kawakami K, Nagao R, Tahara OY, Hamaguchi T, Suzuki T, Dohmae N, Kosumi D, Shen JR, Miyata M, Yonekura K, Kamiya N (2021) Structural implications for a phycobilisome complex from a thermophilic cyanobacterium *Thermosynechococcus vulcanus*, submitted
- Kojima R, Yamamoto H, Azai C, Urugami C, Hashimoto H, Kosumi D, Oh-oka H (2020) Energy transfer and primary charge separation upon selective femtosecond excitation at 810 nm in the reaction center complex from *Heliobacterium modesticaldum*. *J Photochem Photobiol A Chem* 401:112758. <https://doi.org/10.1016/j.jphotochem.2020.112758>
- Kosumi D, Abe K, Karasawa H, Fujiwara M, Cogdell RJ, Hashimoto H, Yoshizawa M (2010) Ultrafast relaxation kinetics of the dark S<sub>1</sub> state in all-trans- $\beta$ -carotene explored by one- and two-photon pump–probe spectroscopy. *Chem Phys* 373:33–37. <https://doi.org/10.1016/j.chemphys.2009.12.013>
- Kromdijk J, Glowacka K, Leonelli L, Gabilly ST, Iwai M, Niyogi KK, Long SP (2016) Improving photosynthesis and crop productivity by accelerating recovery from photoprotection. *Science* 354:857–861. <https://doi.org/10.1126/science.1242321>
- Li Z, Wakao S, Fischer BB, Niyogi KK (2009) Sensing and responding to excess light. *Annu Rev Plant Biol* 60:239–260. <https://doi.org/10.1146/annurev-arplant.58.032806.103844>
- Liu H, Zhang H, Niedzwiedzki DM, Prado M, He G, Gross ML, Blankenship RE (2013) Phycobilisomes supply excitations to both photosystems in a megacomplex in cyanobacteria. *Science* 342:1104–1107. <https://doi.org/10.1126/science.1242321>
- Ma J, You X, Sun S, Wang X, Qin S, Sui S-F (2020) Structural basis of energy transfer in *Porphyridium purpureum* phycobilisome. *Nature* 579:146–151. <https://doi.org/10.1038/s41586-020-2020-7>
- MacColl R (1998) Cyanobacterial Phycobilisomes. *J Struct Biol* 124:311–334. <https://doi.org/10.1006/jsbi.1998.4062>
- MacColl R (2004) Allophycocyanin and energy transfer. *Biochim Biophys Acta* 1657:73–81. <https://doi.org/10.1016/j.bbabi.2004.04.005>
- Marx A, Adir N (2013) Allophycocyanin and phycocyanin crystal structures reveal facets of phycobilisome assembly. *Biochim Biophys Acta* 1827:311–318. <https://doi.org/10.1016/j.bbabi.2012.11.006>
- Maxson P, Sauer K, Zhou JH, Bryant DA, Glazer AN (1989) Spectroscopic studies of cyanobacterial phycobilisomes lacking core polypeptides. *Biochim Biophys Acta* 977:40–51. [https://doi.org/10.1016/s0005-2728\(89\)80007-6](https://doi.org/10.1016/s0005-2728(89)80007-6)
- Muller P, Li XP, Niyogi KK (2001) Non-photochemical quenching A Response to Excess Light Energy. *Plant Physiol* 125:1558–1566. <https://doi.org/10.1104/pp.125.4.1558>
- Nganou AC, David L, Adir N, Pouhe D, Deen MJ, Mkandawire M (2015) Evidence of additional excitation energy transfer pathways in the phycobiliprotein antenna system of *Acaryochloris marina*. *Photochem Photobiol Sci* 14:429–438. <https://doi.org/10.1039/c4pp00352g>
- Nganou C, David L, Adir N, Mkandawire M (2016) Linker proteins enable ultrafast excitation energy transfer in the phycobilisome antenna system of *Thermosynechococcus vulcanus*. *Photochem Photobiol Sci* 15:31–44. <https://doi.org/10.1039/c5pp00285k>
- Niedzwiedzki DM, Bar-Zvi S, Blankenship RE, Adir N (2019) Mapping the excitation energy migration pathways in phycobilisomes from the cyanobacterium *Acaryochloris marina*. *Biochim Biophys Acta* 1860:286–296. <https://doi.org/10.1016/j.bbabi.2019.01.002>
- Peng PP et al (2014) The structure of allophycocyanin B from *Synechocystis* PCC 6803 reveals the structural basis for the extreme redshift of the terminal emitter in phycobilisomes. *Biol Crystallogr* 70:2558–2569. <https://doi.org/10.1107/S1399004714015776>
- Petrasek Z et al (2005) Excitation energy transfer from phycobiliprotein to chlorophyll *d* in intact cells of *acaryochloris marina* studied by time- and wavelength-resolved fluorescence spectroscopy. *Photochem Photobiol Sci off J Eur Photochem Assoc Eur Soc Photobiol* 4:1016–1022. <https://doi.org/10.1039/b512350j>
- Pieper J, Ratsep M, Golub M, Schmitt FJ, Artene P, Eckert HJ (2017) Excitation energy transfer in phycobiliproteins of the cyanobacterium *Acaryochloris marina* investigated by spectral hole burning. *Photosynth Res* 133:225–234. <https://doi.org/10.1007/s1120-017-0396-5>
- Sandström Å, Gillbro T, Sundström V, Fischer R, Scheer H (1988) Picosecond time-resolved energy transfer within C-phycocyanin aggregates of *Mastigocladus laminosus*. *Biochim Biophys Acta* 933:42–53. [https://doi.org/10.1016/0005-2728\(88\)90054-0](https://doi.org/10.1016/0005-2728(88)90054-0)

- Shen J-R, Kawakami K, Koike H (2011) Purification and crystallization of oxygen-evolving photosystem ii core complex from thermophilic cyanobacteria. In: Carpentier R (ed) Photosynthesis research protocols. Humana Press, Totowa, NJ, pp 41–51. [https://doi.org/10.1007/978-1-60761-925-3\\_5](https://doi.org/10.1007/978-1-60761-925-3_5)
- Stadnichuk IN, Krasil'nikov PM, Zlenko DV (2015a) Cyanobacterial Phycobilisomes and Phycobiliproteins. *Microbiology* 84:131–143. <https://doi.org/10.1134/S0026261715020150>
- Stadnichuk VI, Lukashov EP, Yanyushin MF, Zlenko DV, Muronez EM, Stadnichuk IN, Krasilnikov PM (2015b) Energy transfer pathways among phycobilin chromophores and fluorescence emission spectra of the phycobilisome core at 293 and 77 K *Doklady. Biochem Biophys* 465:401–405. <https://doi.org/10.1134/S1607672915060149>
- Stec B, Troxler RF, Teeter MM (1999) Crystal structure of C-phyco-cyanin from *Cyanidium caldarium* provides a new perspective on phycobilisome assembly. *Biophys J* 76:2912–2921. [https://doi.org/10.1016/S0006-3495\(99\)77446-1](https://doi.org/10.1016/S0006-3495(99)77446-1)
- van Stokkum IHM, Gwizdala M, Tian L, Snellenburg JJ, van Grondelle R, van Amerongen H, Berera R (2018) A functional compartmental model of the *Synechocystis* PCC 6803 phycobilisome. *Photosynth Res* 135:87–102. <https://doi.org/10.1007/s11120-017-0424-5>
- Tang K et al (2015) The terminal phycobilisome emitter, LCM: A light-harvesting pigment with a phytochrome chromophore. *Proc Natl Acad Sci USA* 112:15880–15885. <https://doi.org/10.1073/pnas.1519177113>
- Tian L, Gwizdala M, van Stokkum IH, Koehorst RB, Kirilovsky D, van Amerongen H (2012) Picosecond kinetics of light harvesting and photoprotective quenching in wild-type and mutant phycobilisomes isolated from the cyanobacterium *Synechocystis* PCC 6803. *Biophys J* 102:1692–1700. <https://doi.org/10.1016/j.bpj.2012.03.008>
- Tian L, van Stokkum IH, Koehorst RB, Jongerius A, Kirilovsky D, van Amerongen H (2011) Site, rate, and mechanism of photoprotective quenching in cyanobacteria. *J Am Chem Soc* 133:18304–18311. <https://doi.org/10.1021/ja206414m>
- Wahadoszamen M, Kruger TPJ, Ara AM, van Grondelle R, Gwizdala M (2020) Charge transfer states in phycobilisomes. *Biochim Biophys Acta Bioenerg* 1861:148187. <https://doi.org/10.1016/j.bbabi.2020.148187>
- Wang Q, Moerner WE (2015) Dissecting pigment architecture of individual photosynthetic antenna complexes in solution. *Proc Natl Acad Sci U S A* 112:13880–13885. <https://doi.org/10.1073/pnas.1514027112>
- Watanabe M, Ikeuchi M (2013) Phycobilisome: architecture of a light-harvesting supercomplex. *Photosynth Res* 116:265–276. <https://doi.org/10.1007/s11120-013-9905-3>
- Womick JM, Moran AM (2009) Nature of excited states and relaxation mechanisms in C-phyco-cyanin. *J Phys Chem B* 113:15771–15782. <https://doi.org/10.1021/jp908093x>
- Wong CY et al (2012) Electronic coherence lineshapes reveal hidden excitonic correlations in photosynthetic light harvesting. *Nat Chem* 4:396–404. <https://doi.org/10.1038/nchem.1302>
- Yamamoto H, Taomoto M, Ito A, Kosumi D (2020) Electron-transfer behaviors between photoexcited metal complex and methyl viologen codoped in ionic nanospheres. *J Photochem Photobiol A Chem* 401:112771. <https://doi.org/10.1016/j.jphotochem.2020.112771>
- Yamanaka G, Glazer AN (1980) dynamic aspects of phycobilisome structure—phycobilisome turnover during nitrogen starvation in *Synechococcus* Sp. *Arch Microbiol* 124:39–47. <https://doi.org/10.1007/Bf00407026>
- Zhang J, Ma J, Liu D, Qin S, Sun S, Zhao J, Sui SF (2017) Structure of phycobilisome from the red alga *Griffithsia pacifica*. *Nature* 551:57–63. <https://doi.org/10.1038/nature24278>
- Zhang JM, Zhao JQ, Jiang LJ, Zheng XG, Zhao FL, Wang HZ (1997) Studies on the energy transfer among the rod-core complex from phycobilisome of *Anabaena variabilis* by time resolved fluorescence emission and anisotropy spectra. *Biochim Biophys Acta* 1320:285–296. [https://doi.org/10.1016/S0005-2728\(97\)00032-7](https://doi.org/10.1016/S0005-2728(97)00032-7)
- Zilinskas BA, Greenwald LS (1986) Phycobilisome Structure and Function. *Photosynth Res* 10:7–35. <https://doi.org/10.1007/bf00024183>

**Publisher's Note** Springer Nature remains neutral with regard to jurisdictional claims in published maps and institutional affiliations.